

Document downloaded from:

<http://hdl.handle.net/10251/163485>

This paper must be cited as:

Macnamara, S.; Blanes Zamora, S.; Iserles, A. (2020). Simulation of bimolecular reactions: Numerical challenges with the graph Laplacian. *The ANZIAM Journal*. 61:1-16.
<https://doi.org/10.21914/anziamj.v61i0.15169>



The final publication is available at

<https://doi.org/10.21914/anziamj.v61i0.15169>

Copyright Cambridge University Press

Additional Information

Simulation of bimolecular reactions: numerical challenges with the Graph Laplacian

S. Macnamara¹

Sergio Blanes²

Arieh Iserles³

2020

Abstract

An important framework for modelling and simulation of chemical reactions is a Markov process sometimes known as a master equation. Explicit solutions of master equations are rare; in general the explicit solution of the governing master equation for a bimolecular reaction remains an open question. We point out that a solution is possible in special cases for some chemical experiments reported in the literature. The method of solution is diagonalization. The crucial class of matrices are non-symmetric graph Laplacians. We illustrate how standard numerical algorithms for eigenvalues fail for this application. We propose a novel way to explore the pseudospectra for this class of applications, and illustrate our proposal by Monte Carlo. Finally, we apply the Magnus expansion, which provides a method of simulation when rates change in time. Again the Graph Laplacian structure presents some unique issues: standard numerical methods of more than second order fail to preserve positivity. We therefore propose a method that can achieve fourth order accuracy, and maintain positivity.

Contents

1	Introduction	2
2	Exact solutions, spectra and pseudospectra	3
3	Application of the Magnus expansion	6
4	Conclusions	8

1 Introduction

This article is motivated by the experiments in a Harvard chemistry lab with a so-called Dimple Machine, described in “Mass action at the single-molecule level,” by Shon & Cohen [8], and on the website <http://cohenweb.rc.fas.harvard.edu/Research/TrapSingMol/DimpleMachine.htm>. Sections 1.2 & 1.6 of the associated PhD thesis describe the way that Markov processes provide a mathematical framework for models of these chemical reactions [9], and we will use the same mathematical models here. Briefly, we study what is sometimes termed a master equation

$$\frac{d}{dt}p = \mathbb{A}p \quad \text{with solution} \quad p(t) = \exp(\mathbb{A}t)p(0). \quad (1)$$

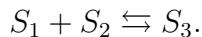
Here the i th component of the vector $p \in \mathbb{R}^n$ records the probability of being in state i . A state is defined by the integer number of molecules of each type of chemical species. The matrix \mathbb{A} must be an example of a (typically non-symmetric) **graph Laplacian**, which is defined by the properties that off-diagonal entries are zero or positive, and each column sums to zero:

1. $a_{ij} \geq 0$, and
2. $a_{jj} = -\sum_{i \neq j} a_{ij}$.

A comparison of these mathematical models with experiments is shown in Figure 4 of [8] – these chemical reactions are described extremely well by this theory!

In very special cases a governing master equation has an exact solution, in which case the matrix exponential appearing in (1) can be made more explicit. For example, for a model of monomolecular reactions, exact solutions, and eigenvalues of associated matrix, have been found by Iserles & Macnamara [3], where more details are given. That model is an example of a class of master equations in which the family of binomial distributions form a one-dimensional *invariant manifold*, and it has important applications to ion channel kinetics [2].

For the rest of this article we will concentrate on the bimolecular reaction



We assume the initial state is $(m_1, m_2, 0)$ molecules of each of the three species, S_1, S_2, S_3 , with $m_2 \geq m_1$. With $n = m_1 + 1$, this is modelled by the $n \times n$ tridiagonal matrix

$$\mathbb{A}_{i,j} = \begin{cases} c_2(j-1), & i = j-1, \\ -c_2(j-1) - c_1(m_1 - j + 1)(m_2 - j + 1) & i = j, \\ c_1(m_1 - j + 1)(m_2 - j + 1), & i = j+1. \end{cases} \quad (2)$$

For simplicity, we give examples for the special case that $m_1 = m_2 = m$, although our methods work more generally. This special case models the experiments in Figure 4(f) of [8], which in that figure are labelled $(N_R, N_G) = (1, 1)$ (corresponding here to $m = 1$), $(2, 2)$ ($m = 2$), and $(3, 3)$ ($m = 3$), for example. They denote red and green monomers by N_R and N_G , which we have here generically denoted S_1 and S_2 . Here we let c_1, c_2 denote rate constants, which are denoted k_{on} and k_{off} with appropriate units in Table 1 of [8], but the exact scalings depend on things such as the volume of the reacting vessel, which will not be considered here, and which do not effect the results we describe, which are generally applicable to this class of models.

2 Exact solutions, spectra and pseudospectra

We examine the spectra and pseudospectra of the model \mathbb{A} in (2). Then we outline a procedure for exact diagonalization, which leads to more explicit solutions via $\exp(\mathbb{A}t) = V \text{diag}(e^{\lambda_0}, \dots, e^{\lambda_m}) V^{-1}$ (albeit the algebraic expressions for V^{-1} could quickly become unwieldy). It is helpful to know that, surprisingly, the non-symmetric matrix does not have complex eigenvalues.

Lemma 1. *The eigenvalues of the non-symmetric matrix (2) representing the bimolecular reaction are purely real.*

Here we use the same method of proof described in [10, Section 12], specialised to this particular application of the Dimple Machine.

Proof: Let $d_1 = 1$. Recursively define $d_{i+1} = \sqrt{\frac{c_2(j-1)}{c_1(m_1-j+1)(m_2-j+1)}} d_i$. Define the diagonal matrix \mathbb{D} with diagonal $d_{ii} = d_i$. Direct matrix multiplication confirms that $\mathbb{D}\mathbb{A}\mathbb{D}^{-1}$ is a symmetric matrix, so by the Spectral Theorem, eigenvalues are real. Hence the eigenvalues of \mathbb{A} are also real, because \mathbb{A} is similar to $\mathbb{D}\mathbb{A}\mathbb{D}^{-1}$. ♠

Remark. Numerical calculation of eigenvalues (in all numerical software, including MATLAB) of this matrix (2), say for $m > 100$, produces complex numbers, with imaginary components of significant magnitude. See Figure 1. The Lemma shows such numerical calculations are wrong. This numerical issue is related to Twisted Toeplitz matrices and the *pseudospectra* [10]. Pseudospectra and other computational issues for this class of problems more generally are discussed in [4, 6, 5, 7], and references therein.

Figure 1 also shows numerical estimates of eigenvalues for a perturbed version of the matrix (2). These perturbed points are a very crude estimate of the pseudospectra of the matrix, visualised as a dot cloud. However, there

is an important difference between what is computed here in Figure 1 and the standard definition of the pseudospectra in the literature. For $\epsilon > 0$, one equivalent definition of the ϵ -pseudospectra of A is the set (in the complex plane) of eigenvalues of some perturbed matrix $A + E$:

$$\{\lambda \in \mathbb{C} : (A + E)v = \lambda v, \quad E \in \mathbb{C}^{n \times n}, \|E\| < \epsilon\}.$$

That formal notion of the pseudospectra has a drawback for these applications because it corresponds to perturbing entries in the matrix A in a way that does not have a physical interpretation in the probabilistic model. In particular, the perturbations permit:

1. negative off-diagonal entries,
2. columns with non-zero sum, and
3. zero entries becoming non-zero.

The first two points violate the Graph Laplacian structure, and third point is not allowed according the chemical reactions being modelled by the matrix. For example, changing entries beyond the tridiagonal structure, in this application, would correspond to changes in state that are impossible with only a bimolecular chemical reaction.

Therefore, to explore the pseudospectra in a way that avoids these three types of violations of the underlying model, here we propose instead to perturb only the positive entries of the matrix (2), and in a way that respects the Graph Laplacian structure and chemical structure. This perturbation is done by adding the absolute value of independent and identically distributed (i.i.d) samples from the standard normal distribution to each positive entry of (2), and then adjusting the negative main diagonal entries to preserve the graph Laplacian property. Figure 1 illustrates an example of our proposal. Visually, this appears very similar to what one might obtain by the usual pseudospectra. A plausible explanation of that similarity is that the figure is still computed by standard eigenvalue algorithms, which can only return estimates that approximately correspond to the usual pseudospectra of the input matrix to the algorithm. (And although the class of matrices being input are structurally different to what is usually input, they are intuitively still ‘close’).

Remark. Finding eigenvalues of a 4×4 version of the matrix (2) (corresponding to $m = 3$ and the (3, 3) case in the experiments of Figure 4(f) of [8]), with symbolic software in Wolfram Alpha (<https://www.wolframalpha.com/>, accessed 20/02/2020) produces a complicated expression, involving

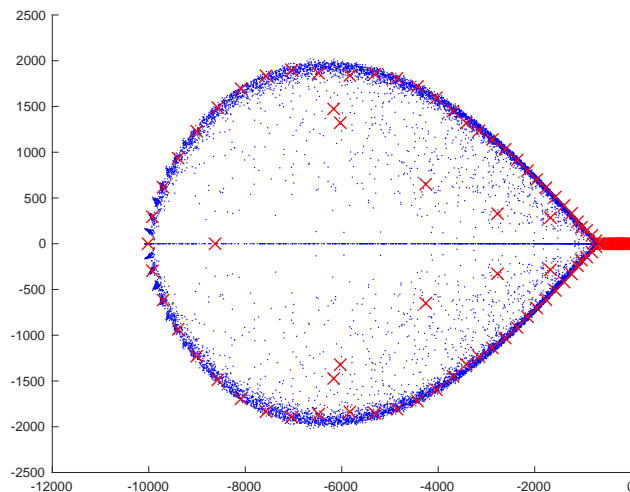


Figure 1: Numerical estimates of the eigenvalues of a 100×100 instance of the matrix (2) with $c_1 = c_2 = 1, m = 99$, computed with the numerical software MATLAB, plotted ('x') in the complex plane. Numerical estimates for 200 randomly perturbed versions of the matrix in (2) are also plotted ('.') According to the Lemma, exact eigenvalues are real. So complex eigenvalues here are wrong: numerical methods fail on this class of Graph Laplacians.

imaginary units: $-\frac{1}{6^3\sqrt{2}}(1 \pm i\sqrt{3})(\sqrt{4(-3c_2^2 + 6c_1c_2 - 49c_1^2)})^3 + \dots$. Presumably this is an artefact of the Wolfram Alpha software using Cardano's formula for an associated cubic. If not aware of the Lemma, then a naive user of symbolic algebra software might easily be misled.

From standard theory of Markov processes it is known that matrices such as (2) have a unique zero eigenvalue, and that all other eigenvalues have negative real part. Together with the lemma, we see that all other eigenvalues are negative.

After factoring out the zero eigenvalue, the characteristic polynomial is reduced in degree by one. Hence we can find the eigenvalues of the 3×3 case with the quadratic formula, and the 4×4 case with Cardano's formula for the cubic. (And the 5×5 case via formulae for a quartic, but not 6×6 or larger cases, which lead to polynomials of higher degree.) Thus we now have a procedure that finds exact eigenvalues for the cases in all of the experiments in Figure 4(f) of [8], which are there labelled $(N_R, N_G) = (1, 1)$ (corresponding to $m = 1$), $(2, 2)$ (for $m = 2$), and $(3, 3)$ (for $m = 3$).

Having found an eigenvalue, the corresponding right eigenvector can always be found by solving $\mathbb{A}v = \lambda v$, in a recursive way that is analogous to

the method of forward substitution used in Gaussian elimination, to take advantage of the tridiagonal structure. In particular, set $v_1 = 1$, then set $v_2 = v_1(\lambda - a_{11})/a_{12}$, and then recursively

$$v_{i+1} = (-a_{i,i-1}v_{i-1} + (\lambda - a_{ii})v_i)/a_{i,i+1}.$$

Thus we have a procedure to exactly diagonalise the examples in all of the experiments in Figure 4(f) of [8], mentioned above.

Note that the stationary distribution (the right eigenvector for $\lambda = 0$) can always be found this way, and this distribution is well known for this class of bimolecular models (see, e.g. sections 1.2 & 1.6 of [9]). Indeed, even more generally than the class of models we study in this article, for all matrices of the Graph Laplacian type, there are known formulae, according to the Matrix-Tree Theorem, for the vector in the null space.

As a very simple illustrative example with $\lambda_0 = 0$, $\lambda_1 = -(c_1 + c_2)$, an exact diagonalization for the $m = 1$ Figure 4(f) of [8] case is

$$\begin{pmatrix} -c_1 & c_2 \\ c_1 & -c_2 \end{pmatrix} = \frac{1}{\sqrt{|\lambda_1|}} \begin{pmatrix} c_2 & 1 \\ c_1 & -1 \end{pmatrix} \begin{pmatrix} \lambda_0 & 0 \\ 0 & \lambda_1 \end{pmatrix} \begin{pmatrix} 1 & 1 \\ c_1 & -c_2 \end{pmatrix} \frac{1}{\sqrt{|\lambda_1|}}$$

As another example, exact eigenvalues and eigenvectors for the $m = 2$ case in experiments in Figure 4(f) of [8] are

$$\lambda_0 = 0 \quad \text{and} \quad v_0 = (1, 4c_1/c_2, 2c_1^2/c_2^2)^\top$$

and

$$\lambda_{\pm} = \frac{1}{2} \left(-5c_1 - 3c_2 \pm \sqrt{c_2^2 - 2c_2c_1 + 9c_1^2} \right),$$

$$v_{\pm} = (1, (4c_1 + \lambda_{\pm})/c_2, c_1(4c_1 + \lambda_{\pm})/(c_2(2c_2 + \lambda_{\pm})))^\top.$$

The autocorrelation function in equation (5) of [8] is used to estimate the rate constants from observations of the experiments. That autocorrelation involves the matrix exponential of (1), and in the 2×2 case this is available as an algebraic expression as noted above, but for larger matrices this matrix exponential is numerically estimated in [8]. The procedure for exact diagonalizations we describe above, for say the 3×3 case, would allow expressions for the matrix exponential to be found without resorting to numerical calculation - allowing the dependence on parameters to be made explicit.

3 Application of the Magnus expansion

We now consider the case that the rate ‘constants’ $c_1 = c_1(t)$ and $c_2 = c_2(t)$ in (2) are in fact time dependent, to handle experiments that can perturb

these rates. Instead of (1), we now have

$$\frac{d}{dt}\mathbf{p} = \mathbb{A}(t)\mathbf{p} \quad \text{with solution} \quad \mathbf{p}(t) = \exp(\Omega(t))\mathbf{p}(0). \quad (3)$$

Here, $\Omega(t)$ is given by the Magnus expansion [1, 3]:

$$\Omega(t) = \int_0^t \mathbb{A}(s)ds - \frac{1}{2} \int_0^t \left[\int_0^s \mathbb{A}(r)dr, \mathbb{A}(s) \right] ds + \dots \quad (4)$$

with all higher order terms (not shown) involving commutators.

It is known that a fourth order method can be obtained by including just one commutator: $\sigma = \frac{1}{2}h(A_1 + A_2) + \frac{\sqrt{3}}{12}h^2[A_2, A_1]$. Here $A_1 = \mathbb{A}(t + (1/2 - \sqrt{3}/6)h)$ and $A_2 = \mathbb{A}(t + (1/2 + \sqrt{3}/6)h)$ are evaluated at Gauss quadrature points, and we take a time step h in the numerical scheme via

$$\hat{p}(t+h) = \exp(\sigma)\hat{p}(t). \quad (5)$$

To exemplify how to specialise this method to the bimolecular reaction, let us suppose that $c_1 = c_1(t)$, and c_2 is constant. Then the commutators can be simplified. For example, in the 3×3 case ($m = 2$), we have $\mathbb{A}(t) = c_1(t)M + N$ where M and N (involving only c_2) are constant matrices. Hence

$$[\mathbb{A}(t_1), \mathbb{A}(t_2)] = (c_1(t_1) - c_1(t_2))[M, N].$$

The point is that the commutator $[\mathbb{A}(t_1), \mathbb{A}(t_2)]$ required by the Magnus expansion and the numerical scheme, involves *constant* matrices. Thus $[M, N]$ can be precomputed off-line, and then all other computations only involve the scalar function $c_1(t)$, which represents a considerable numerical savings.

The advantage of including the commutator is the significant increase in the order of accuracy. For our particular class of problems, a disadvantage is that *a commutator of two graph Laplacian matrices is not usually again a graph Laplacian*. To illustrate this issue with our running example, notice that up to the scalar factor $(c_1(t_1) - c_1(t_2))$, we have

$$[\mathbb{A}(t_1), \mathbb{A}(t_2)] \propto \pm[M, N] = \begin{pmatrix} -4c_2 & -5c_2 & 0 \\ 4c_2 & 2c_2 & -2c_2 \\ 0 & c_2 & 2c_2 \end{pmatrix}$$

but this evidently does not have the right pattern of signs for a Graph Laplacian. This matters because graph Laplacians have the special property that all entries of $\exp(A)$ are nonnegative and columns are probability vectors, which is important to the probabilistic interpretation of the model. Unfortunately, the commutator does not have the same pattern of signs as the matrix \mathbb{A} , and although it is fourth order, the numerical method (5) could produce negative numbers (while the true solution is positive).

Fourth-order commutator-free quasi-Magnus integrator To avoid the commutators appearing in the exponent of the Magnus integrators that are not graph Laplacian matrices, we now consider commutator-free quasi-Magnus integrators. For example, consider the averaged matrices

$$\sigma_1 = \frac{1}{2}h(\alpha A_1 + \beta A_2), \quad \sigma_2 = \frac{1}{2}h(\beta A_1 + \alpha A_2),$$

with $A_1 = \mathbb{A}(t + (1/2 - \sqrt{3}/6)h)$ and $A_2 = \mathbb{A}(t + (1/2 + \sqrt{3}/6)h)$ and

$$\alpha = \frac{1}{2} + \frac{\sqrt{3}}{3}, \quad \beta = \frac{1}{2} - \frac{\sqrt{3}}{3}.$$

Note that $\alpha + \beta = 1$, $\beta < 0$, $\frac{\alpha}{|\beta|} = 7 + 4\sqrt{3} \simeq 14$, the point is that β is negative, but much smaller than α . Then, unless $A(t)$ changes with t suddenly, σ_1 and σ_2 will remain graph Laplacian matrices.

A fourth-order integrator in the time step h is given by the numerical scheme (see [1] and references therein)

$$\hat{p}(t+h) = \exp(\sigma_2) \exp(\sigma_1) \hat{p}(t). \quad (6)$$

Each exponential can be seen as a scheme to advance a half step with an averaged method followed by the averaged adjoint method, such that at the result is accurate up to order four.

For our illustrative example in which $c_1 = c_1(t)$ while c_2 is constant, the only constraint for σ_1, σ_2 to be graph Laplacian matrices is that

$$\max \left\{ \frac{c_1(t_1)}{c_1(t_2)}, \frac{c_1(t_2)}{c_1(t_1)} \right\} < 7 + 4\sqrt{3} \simeq 14.$$

If $c_1(t)$ is a smooth function, this is a condition that should be satisfied for all time steps of practical interest. Moreover, this condition can always be guaranteed with simple adaptive time stepping.

4 Conclusions

We have applied techniques for graph Laplacians to a particular application that is motivated by single molecule technology and experiments with the Dimple Machine [8]. We have given reasons why the usual way of studying the pseudospectra has a drawback for Graph Laplacians for these applications, and therefore we have proposed instead a different way to interrogate (an approximation to) the pseudospectra, which we illustrate with the Monte Carlo dot cloud of Figure 1.

We explained that exact diagonalizations are possible via the procedure we exemplified for some of the experiments, which can give exact solutions. However, the exact solution to the bimolecular master equation with $m = 5$ or more molecules of each species S_1, S_2 , and associated eigenvalues of (2), remains an important open question.

Finally, we suggest how the Magnus expansion can be applied to this particular application for simulations of bimolecular reactions when rates vary in time. The recurring theme of the article is the Graph Laplacian structure, and again this issue manifests itself in the commutators arising in that infinite expansion. Standard numerical methods are not able to respect key properties of the solution, such as non-negativity. We address this issue by showing how a fourth order method can be achieved while simultaneously maintaining positivity. Preserving the graph Laplacian structure and associated qualitative properties in numerical schemes is a much wider issue than only the application we focused on here, which represents an important future challenge.

Acknowledgements We thank the organisers and delegates of the Canberra 2019 EMAC conference for helpful discussions about graph Laplacians.

References

- [1] Sergio Blanes et al. “The Magnus expansion and some of its applications”. In: *Physics reports* 470.5-6 (2009), pp. 151–238. DOI: 10.1016/j.physrep.2008.11.001 (cit. on pp. 7, 8).
- [2] Berton A. Earnshaw and James P. Keener. “Invariant Manifolds of Binomial-Like Nonautonomous Master Equations”. In: *SIAM Journal on Applied Dynamical Systems* 9.2 (2010), pp. 568–588. DOI: 10.1137/090759689 (cit. on p. 2).
- [3] A. Iserles and S. MacNamara. “Applications of Magnus expansions and pseudospectra to Markov processes”. In: *European Journal of Applied Mathematics* 30.2 (2019), 400–425. DOI: 10.1017/S0956792518000177 (cit. on pp. 2, 7).
- [4] Shev MacNamara. “Cauchy integrals for computational solutions of master equations”. In: *ANZIAM Journal* 56 (2015), pp. 32–51. DOI: 10.21914/anziamj.v56i0.9345 (cit. on p. 3).

- [5] Shev MacNamara, Kevin Burrage, and Roger B. Sidje. “Multiscale Modeling of Chemical Kinetics via the Master Equation”. In: *SIAM Multiscale Model. & Sim.* 6.4 (2008), pp. 1146–1168. DOI: 10.1137/060678154 (cit. on p. 3).
- [6] Shev MacNamara, William McLean, and Kevin Burrage. “Wider Contours and Adaptive Contours”. In: *2017 MATRIX Annals*. Ed. by Jan de Gier, Cheryl E. Praeger, and Terence Tao. Springer International Publishing, 2019, pp. 79–98. DOI: 10.1007/978-3-030-04161-8_7 (cit. on p. 3).
- [7] Shev MacNamara et al. “Stochastic chemical kinetics and the total quasi-steady-state assumption: application to the stochastic simulation algorithm and chemical master equation”. In: *J. Chem. Phys.* 129 (2008), p. 095105. DOI: 10.1063/1.2971036 (cit. on p. 3).
- [8] M. J. Shon and A. E. Cohen. “Mass action at the single-molecule level”. In: *J. Am. Chem. Soc.* 134.35 (2012), pp. 14618–14623. DOI: 10.1021/ja3062425 (cit. on pp. 2–6, 8).
- [9] Min Ju Shon. “Trapping and manipulating single molecules of DNA”. PhD thesis. Harvard University, 2014 (cit. on pp. 2, 6).
- [10] L. N. Trefethen and M. Embree. *Spectra and Pseudospectra: The Behavior of Nonnormal Matrices and Operators*. Princeton University Press, 2005 (cit. on p. 3).

Author addresses

1. **S. Macnamara**, Australian Research Council Centre of Excellence for Mathematical and Statistical Frontiers (ACEMS), School of Mathematical and Physical Sciences, University of Technology Sydney, NSW 2007, AUSTRALIA.
mailto:shev.macnamara@uts.edu.au
2. **Sergio Blanes**, Instituto de Matemática Multidisciplinar, Universitat Politècnica de València, Edificio 8-G, piso 2, Camino de Vera s/n, 46022-Valencia
mailto:serblaza@imm.upv.es
3. **Arieh Iserles**, Department of Applied Mathematics and Mathematical Physics, University of Cambridge, Wilberforce Road, Cambridge CB3 0WA, UK
mailto:a.iserles@damtp.cam.ac.uk